Journal of Catalysis **197,** 58–67 (2001)
doi:10.1006/jcat.2000.3055, available online at http://www.idealibrary.com on IDEAL®

Preparation and Catalytic Properties of Chromium-Containing Mixed Sulfides

A. Thiollier, P. Afanasiev, P. Delichere, and M. Vrinat

Institut de Recherches sur la Catalyse, 2 Avenue A. Einstein, 69626 Villeurbanne Cédex, France

Received May 11, 2000; revised July 24, 2000; accepted August 30, 2000

A series of mixed sulfides dispersions MCr_2S_4 (M = Mn, Fe, Co, Ni, Cu, Zn, Cd, 2Na) has been prepared by means of different chemical methods including sulfidation of mixed oxide dispersions or pyridinium dichromate complexes or reactions in the polysulfide-containing ionic fluxes. The solids were characterized using X-ray diffraction, BET surface measurements, X-ray photoelectron spectroscopy, low-energy ion scattering spectroscopy, and temperature programmed reduction. The catalytic properties of mixed sulfides were determined in the model reactions of tetraline hydrogenation and thiophene hydrodesulfurization. Variations of the specific activity of MCr_2S_4 solids as a function of M in both reactions were similar, having the maxima for the $NiCr_2S_4$ and $CoCr_2S_4$ compounds. Differences in the catalytic activity were correlated with the reducibility, determined as the amount of sulfur removed from the catalysts by hydrogen at 573 K. The reducibility of MCr_2S_4 solids follows from their electronic structure, as illustrated by the extended Hückel calculations.

Key Words: **chromium; mixed sulfides; hydrotreating; reducibility.**

INTRODUCTION

Insight into the catalytic properties of sulfides, the nature of the active sites, and the promotion mechanism remains controversial despite a great effort on this topic made in recent years. Commercial Ni–Mo- and Co–Mo-supported sulfide catalysts are difficult to study because of their excessive complexity. For that reason, the studies of the simple model solids, such as unsupported binary and ternary sulfide dispersions, can be helpful. Various sequences of catalytic activity of binary sulfides have been obtained in several works (1–5). Volcano curves were obtained with the maxima on the elements of group VIII of the periodic table.

The activity sequences of various metal sulfides were correlated with their electronic and/or thermodynamic properties. However, not only the nature of transition metal but also the stoichiometry and crystal structure of sulfides vary within such a series. For example, lamellar MoS_2, cubic face centered NiS, and pyrite-type RuS_2 are widely studied in catalysis sulfides. Comparison of the catalytic properties of these sulfides might be qualitative at best.

A more straightforward discussion of catalytic activity trends might be achieved in the series of similar structures, where elements have the same coordination numbers and oxidation states. Such structures should be as simple as possible and stabile under the reaction conditions. There are several families of sulfides with similar crystal structures, such as those of pyrite FeS_2 (6), nickel arsenide NiAs (7), and spinel $MgAl_2O_4$ (8).

In the present study, dispersions of several mixed sulfides of chromium MCr_2S_4 were prepared and characterized. Their catalytic properties were compared in the model hydrotreating reactions. Most of the solids studied have the spinel structure. This structure is versatile in that it is able to accommodate various metal cations, seeming therefore to be a suitable model system for the fundamental studies.

EXPERIMENTAL

Preparation of Mixed Sulfides

Hydrous oxide precipitates were obtained by adding aqueous ammonia to solutions of mixtures of 0.02 mol $Cr(NO_3)_3 \cdot 9H_2O$ and 0.01 mol of the nitrate or chloride hydrated salt of the second metal (Mn, Fe, Co, Ni, Cu, Zn, Cd), dissolved in 100 ml of distilled water. The precipitates were washed with hot water in a soxhlet apparatus for 4 h and then oven dried in air at 373 K for 12 h. Thermal treatment was performed under nitrogen flow at 773 K for 2 h.

Dichromate pyridinium complexes were obtained by the addition of 50 ml of pyridine to a solution of 0.01 mol $(NH_4)_2Cr_2O_7$ and 0.01 mol of the second metal nitrate in 100 ml of distilled water. Precipitates were aged for 2 days in the solution and then filtered, washed with distilled water, and dried at room temperature for 1 week. Sulfidation was performed in a quartz reactor at 673 or 873 K for 4 h under a flow of 15% H_2S in N_2. Nitrogen was utilized instead of the usually applied hydrogen, because in the presence of the latter pyrophoric solids were obtained.

Preparation of the $NaCrS_2$ compound was performed in the molten mixture S_8 (0.2 mol), Na_2CO_3 (0.04 mol), and $CrCl_3$ (0.01 mol). After the reaction at 623 K for 2 h, the

0021-9517/01 $35.00

product was consequently washed with toluene (to remove sulfur compounds) and water (to remove inorganic compounds) in a soxhlet apparatus.

Characterizations

Chemical analyses were carried out using the atomic emission technique. The X-ray diffraction patterns were obtained on a Siemens D500 diffractometer with Cu$K\alpha$ emission. The diffractograms were analyzed using standard JCPDS files. Specific surface areas were measured by means of low-temperature adsorption of nitrogen and calculated according to the BET equation.

X-ray photoelectron spectroscopy (XPS) studies were performed on a VG Escalab 200R spectrometer using Al$K\alpha$ radiation. The XPS spectra of S 2p, Ni, Co, Zn, Fe, Mn, and Cr 2p were recorded and their binding energies (BE) referred to the energy of the C 1s peak (BE 285.0 eV). Quantification of the surface contents of the elements was done using the sensitivity factors provided with the VG software.

High-resolution electron microscopy was performed with a JEOL 2010 instrument with resolution of 0.2 nm. Scanning electron microscopy (SEM) images were made on a Hitachi S800 apparatus at the CMEAB Center (Claude Bernard University, Lyon).

Due to the unique surface sensitivity of the outermost layer, low-energy ion scattering (LEIS) is a suitable technique for catalyst characterization (9, 10). The analysis of the atomic composition was obtained from the energy distribution of the ions that are back scattered by the surface atoms. The ratio of the energies of the scattered and incident ions is given by

$$E_1/E_0 = \left[\cos\theta + (\gamma^2 - \sin^2\theta)^{1/2}/1+\gamma\right]^2,$$

where θ is the scattering angle and γ is the mass ratio of the surface atom and incident ion. The LEIS experiments were performed with 1 KeV $^4He^+$ ions. The scattering angle was 142° and the current on the target was set to 50 nA. Sample charging effects have been overcome using a flood gun with low-energy electrons. LEIS spectra recorded after a very short time under the ion beam are typical of the very topmost atomic layer of the sample. On the other hand, by increasing the time under the ion beam, one can obtain information on the composition of underlying layers.

Temperature programmed reduction (TPR) was carried out in a quartz reactor. The samples of mixed sulfides (ca 0.1 g) were preheated under nitrogen at 573 K to remove the adsorbed sulfur species and then cooled to room temperature and linearly heated under a hydrogen flow (50 cc min^{-1}) up to 1073 K (5 K/min). Hydrogen sulfide evolved upon reduction was detected by means of a HNU photoionization detector equipped with a 10.2-eV UV light source. The amount of H_2S evolved from the solid was quantified after calibration of the detector with a gas mixture of known H_2S content.

Extended Hückel calculations were carried out using the BICON-EDIT program package (11). Orbital sets were taken from Ref. (12) (Cr, Mn, Fe), (13) (Co), (14) (Cu), (15) (Ni), and (16) (Zn). Density of states (DOS), crystal orbitals overlap population (COOP), Fermi level, and electronic stabilization energy were calculated for several mixed sulfides.

Catalytic Tests

Thiophene hydrodesulfurization (HDS) and tetraline hydrogenation (HYD) reactions were chosen as model reactions for the comparison of catalytic properties. Thiophene HDS was carried out in the vapor phase in a fixed-bed microreactor operated in the dynamic mode at 100 KPa of hydrogen (thiophene pressure: 2.4 KPa, total flow: 6 L/h). The catalyst weight was ca 0.1 g . For the tetraline gas phase HYD, the experimental conditions were so chosen to avoid thermodynamic equilibrium that favors dehydrogenation to form naphthalene. The range of temperatures studied was 523–573 K, the hydrogen pressure 4.5 MPa, the tetraline vapor partial pressure 8.9 KPa, and H_2S pressure 84 KPa. In all catalytic tests, the specific rate was calculated at 573 K in the steady state after 16 h of stream according to the equation

$$A = FX/m,$$

where A is the specific rate ($mol \cdot g^{-1} \cdot s^{-1}$), F is the molar flow rate of the reactant ($mol \cdot s^{-1}$), X is the conversion of reactant, and m is the catalyst weight (g). For this equation to be correct we tried to avoid conversions that were higher than 0.1. In both catalytic tests the products were analyzed by gas chromatography. The relative error on rate measurements was about 10%.

RESULTS AND DISCUSSION

Preparation and Characterization of MCr_2S_4 Dispersions

The preparation technique may have crucial importance, since it determines the amount of impurities in the solid, its morphology, and the number of defects in the structure. These factors may strongly affect the relative catalytic activity in the sequences of sulfides prepared using different methods. Therefore, we prepared several sulfides using a unique procedure under the same conditions to provide the series of catalysts with similar morphologies and other preparation-dependent properties.

Previously reported syntheses of MCr_2S_4 solids were not aimed at catalysis but rather at physical studies, where large crystals are preferred. It was, therefore, our goal to prepare these sulfides in a dispersed state, with the surface areas appropriate for catalytic studies. Only soft chemical methods should be applied, using moderated temperatures, to

avoid extensive sintering. Three methods were utilized, as described below.

Sulfidation of Mixed M(II)–Cr(III) Oxides

The simplest way to obtain dispersed sulfides is to sulfidize finely divided oxide precursors. Here, we prepared mixed chromites or hydrated oxides to use them as precursors. Coprecipitation by aqueous ammonia from the mixtures of aqueous solutions of the corresponding salts yielded green amorphous precipitates. Since the target products are sulfides, we proceeded directly to sulfidizing these precipitates at 673 K. Our goal was achieved if sulfidation at 673 K under a flow of 15% H_2S in N_2 gave mixed sulfides. The sulfidation temperature was otherwise increased to 873 K. If even in this case no mixed sulfide could be observed in XRD, we heated the hydrous oxide at 773 K under nitrogen to obtain a MCr_2O_4 chromite which was then sulfided as described before. Using this procedure, we obtained several different thiospinels (Fig. 1). The preparation conditions and some properties of the solids are listed in Table 1. Surface areas were sufficiently high for a correct comparison of catalytic properties. As expected, surface areas of the same solids prepared at 873 K were lower than that of those sulfided at 673 K.

The morphology of the particles of mixed sulfides was homogeneous as observed by SEM (Fig. 2). All samples obtained from the mixed (or mixed hydrated) oxides consisted of spherical particles with a size of several hundreds of nanometers, corresponding well to the surface area measurements.

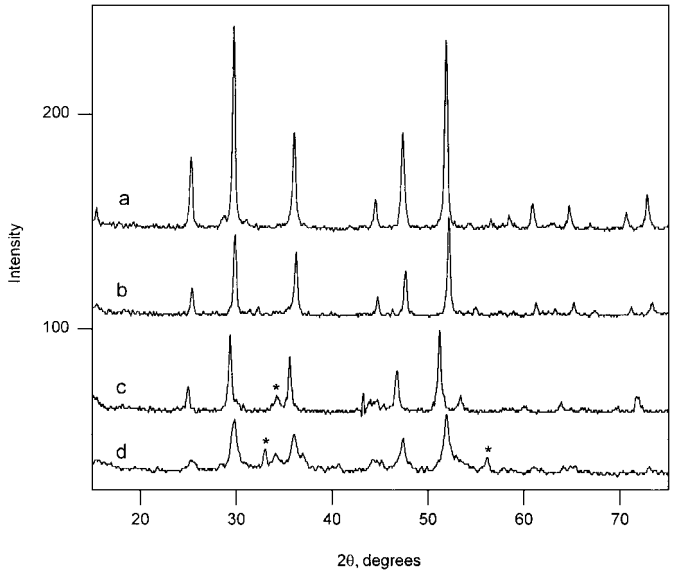

FIG. 1. XRD patterns of MCr_2S_4 sulfides prepared from the sulfidation of mixed oxides $M = Zn$ (a), all peaks—$ZnCr_2S_4$ (JCPDS 16-0507), Co (b), all peaks—$CoCr_2S_4$ (JCPDS 21-0255); Mn (c), all peaks—$MnCr_2S_4$ (JCPDS 36-1441), marked peak—MnS (JCPDS 40-1289); Fe (d), all peaks—$FeCr_2S_4$ (JCPDS 04-0651), marked peak—FeS_2 (JCPDS 37-0475).

TABLE 1

Composition and Surface Area of the Solids Prepared from the Mixed Oxide Precursors

Precursor used	Sulfidation temperature, K	Phase XRD	Chemical composition	S_{sp}, $m^2 \cdot g^{-1}$
Mn–Cr hydrous oxide	873	Spinel	$MnCr_{2.03}S_{4.01}$	13
Fe–Cr hydrous oxide	673	Spinel	$FeCr_{1.87}S_{3.74}$	50
Ni–Cr hydrous oxide	873	Monoclinic	$NiCr_{2.07}S_{4.15}$	13
$CoCr_2O_4$	873	Spinel	$CoCr_{1.99}S_{4.01}$	16
$CuCr_2O_4$	673	Spinel	$CuCr_{2.00}S_{4.01}$	48
$ZnCr_2O_4$	873	Spinel	$ZnCr_{1.99}S_{4.00}$	55
$CdCr_2O_4$	873	Spinel	$CdCr_{2.02}S_{4.02}$	14

Preparations Using the Pyridinium Complexes

For the bivalent metals, the target stoichiometry of the precursor could be provided by dichromate salts MCr_2O_7. However, these salts did not precipitate upon mixing of aqueous solutions of $M(NO_3)_2$ and $(NH_4)_2Cr_2O_7$. If the solution pH was raised by the addition of ammonia, precipitation of $MCrO_4$ monochromates or $M(OH)_2$ hydroxides occurred. However, for several bivalent metals precipitation of dichromate complexes could be performed in the presence of pyridine. Pyridinium complexes of bivalent metals (Mn, Ni, Co, Zn) were formed after addition of an excess of pyridine to the mixed aqueous solutions of $M(NO_3)_2$ and $(NH_4)_2Cr_2O_7$. As found from the chemical analysis, these precipitates were stoichiometric compounds of general formula $MCr_2O_7 \cdot 2NC_5H_5$ (M = Mn, Co, Ni, Zn). The compounds obtained gave complex XRD patterns with several tens of narrow lines, which could not be identified using the standard JCPDS library files. Detailed study of these compounds was beyond the scope of this work.

After being dried, pyridinium complex precursors were sulfided under the H_2S/N_2 flow at 673 K. The sulfidation gave the solids of stoichiometry indicated in Table 2. However, if for Mn and Zn the expected thiospinel phases were formed, for the Co and Ni samples sulfidation at 673 K gave in the XRD patterns only the corresponding pyrite CoS_2 and NiS_2 (Fig. 3), without any signs of the presence of chromium compounds. The XRD peaks were too broad to determine the change of lattice parameters. Further sulfidation at 873 K leads to the thermodynamically stable thiospinel and the monoclinic mixed sulfides for Co and Ni, respectively.

As follows from the data of Table 2, mixed sulfides prepared from the pyridinium complexes at 673 K had slightly higher surface areas than those prepared at the same

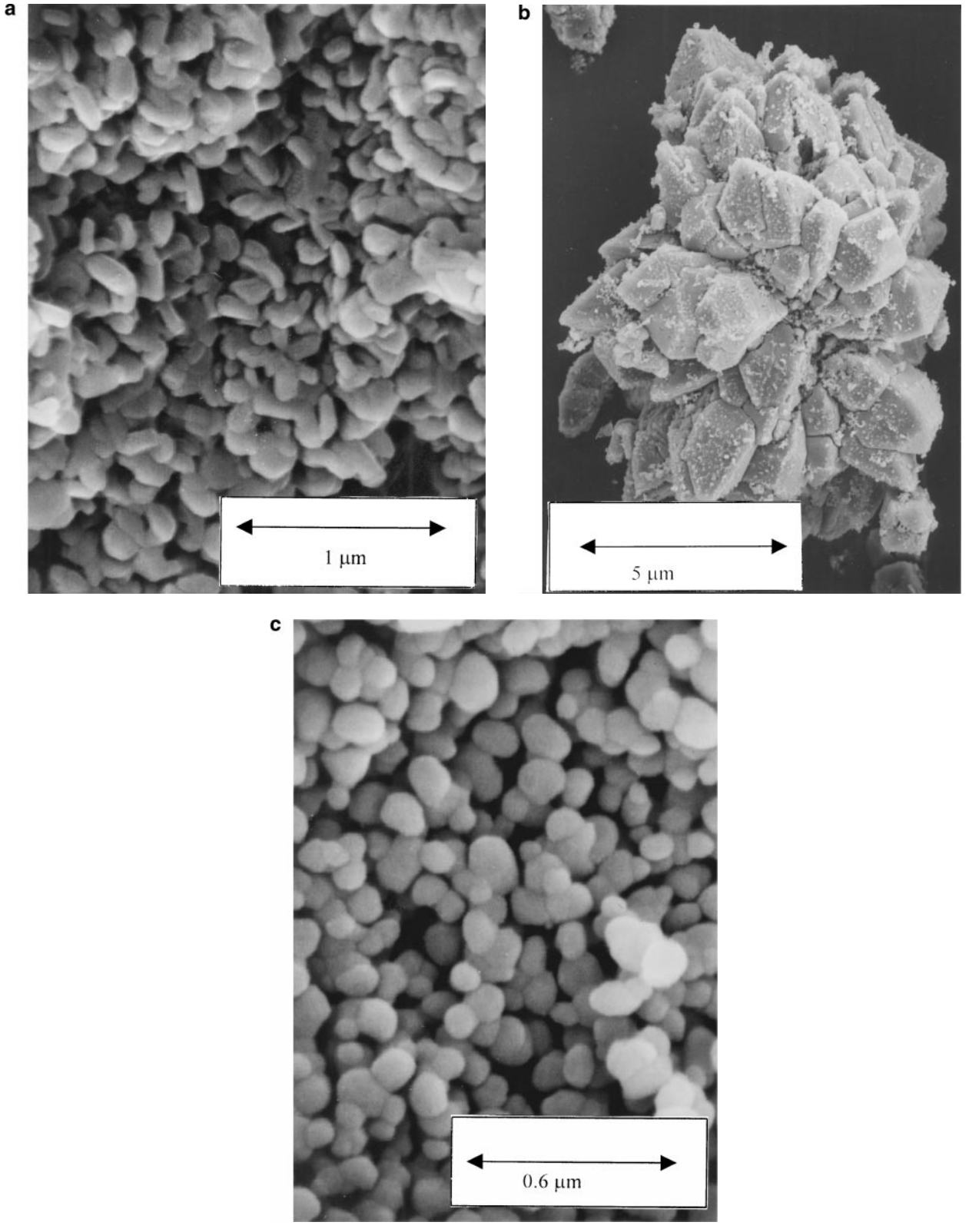

FIG. 2. SEM images of $NaCr_2S_4$ prepared from molten flux, magnification 30 K (a); $MnCr_2S_4$ prepared from the pyridinium complex magnification 600 (b) and the same sample at magnification 50 K (c).

TABLE 2

Properties of MCr_2S_4 Sulfides Prepared from the Pyridinium Dichromate Complexes

Precursor used	Sulfidation temperature, K	Phases, XRD	Chemical composition	S_{sp}, m^2/g
$MnCr_2O_7 \cdot 2Py$	673	Spinel	$MnCr_2S_{4.01}$	63
$NiCr_2O_7 \cdot 2Py$	673	Pyrite	$NiCr_{2.00}S_{4.25}$	110
$NiCr_2O_7 \cdot 2Py$	873	Monoclinic	$NiCr_{2.00}S_{4.15}$	31
$CoCr_2O_7 \cdot 2Py$	673	Pyrite	$CoCr_{1.99}S_{4.01}$	96
$CoCr_2O_7 \cdot 2Py$	873	Spinel	$CoCr_{1.99}S_{4.21}$	22
$ZnCr_2O_4 \cdot 2Py$	673	Spinel	$ZnCr_{1.97}S_{4.02}$	78

temperature from the hydrated oxides. In the SEM images, the solids after sulfidation had the external morphology of the crystalline precursors (Mn compound, Fig. 2b) but at high magnifications they appeared to be composed of the agglomerates of tiny spherical particles of 100- to 200-nm size (Fig. 2c).

Molten Polysulfide Flux Synthesis

Reactions of molten sulfide fluxes have been used for syntheses of the mixed sulfides of main and transition group elements. These solids often contain in their structure the alkali metal cations included in the melt (17). In the present work, a mixed sulfide with Na was obtained from the reaction of Na_2CO_3 and $CrCl_3$ in molten sulfur, according to the reaction

$$3Na_2CO_3 + 3S + CrCl_3 \Rightarrow 3NaCl + NaCrS_2 + Na_2SO_4 + 2CO_2 + CO. \quad [1]$$

The solid product had a specific surface area of 51 $m^2 \cdot g^{-1}$ and consisted of spherical particles. Its chemical composition and XRD pattern corresponded fairly to those of the $NaCrS_2$ solid (JCPDS 10-0292).

In conclusion, a series of eight MCr_2S_4 dispersions has been synthesized, six of which belong to the thiospinel family (M = Mn, Fe, Co, Cu, Zn, Cd), whereas two others (2Na, Ni) have different structures. In the trigonal $NaCrS_2$ compound (18) the coordination numbers of chromium and sodium are 6 and 4, respectively, similarly to thiospinels, but in the monoclinic $NiCr_2S_4$ (19) the coordination number of Ni is equal to that of chromium (CN = 6). However, despite this difference, we included the nonspinel compounds in the mixed sulfides series.

Catalytic Properties

The results of catalytic tests are presented in Figs. 4 and 5. All of the samples slightly activate during the catalytic tests, with reaction rates stabilizing after 10–15 h of reaction. The selectivities in both reactions were similar for all samples, therefore we compare just the reaction rates. In the case of thiophene, selectivity in tetrahydothiophene was negligible, therefore the HDS rate exclusively was measured. For both HDS and HYD reactions, volcano curves were obtained with the maxima for Ni solids. Na-containing sulfide had almost zero activity, whereas other solids show measurable values, sometimes comparable to that of the unsupported MoS_2 (the catalytic activity of MoS_2 in HDS of thiophene is 0.85 10^6 mol min^{-1} m^{-2} and in HYD of tetraline is 0.39 10^6 mol min^{-1} m^{-2}). The HYD/HDS activity ratio was higher for the $NiCr_2S_4$ solid than for the molybdenum sulfide reference, in agreement with our previous finding

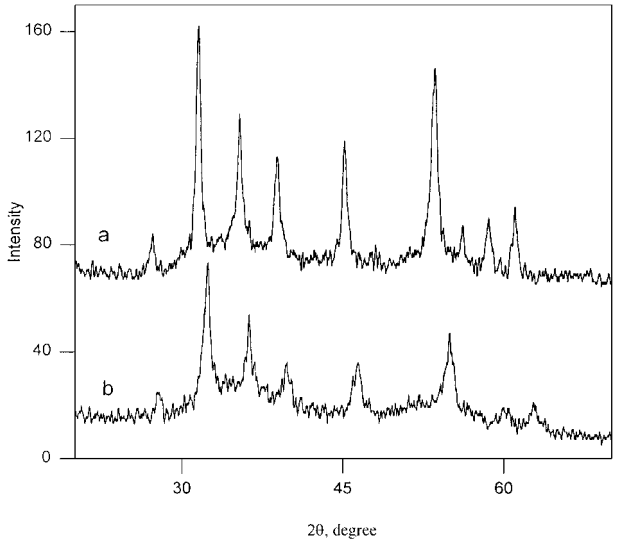

FIG. 3. XRD patterns of $CoCr_2S_4$ solid (a) (all peaks—CoS_2, JCPDS 41-1471); and $NiCr_2S_4$ solid, (b) (all peaks—NiS_2, JCPDS 11-0099). Solids were prepared from the pyridinium complexes by sulfidation in an N_2–H_2S mixture at 673 K.

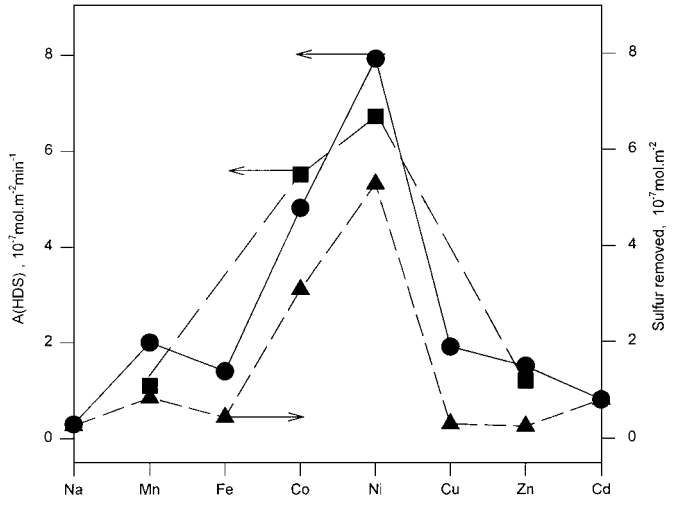

FIG. 4. Catalytic activity of the MCr_2S_4 solids at 573 K in the reaction of HDS of thiophene (circles, oxide derived samples; squares, pyridinium complexes derived catalysts) and the amount of sulfur removed at 573 K (triangles).

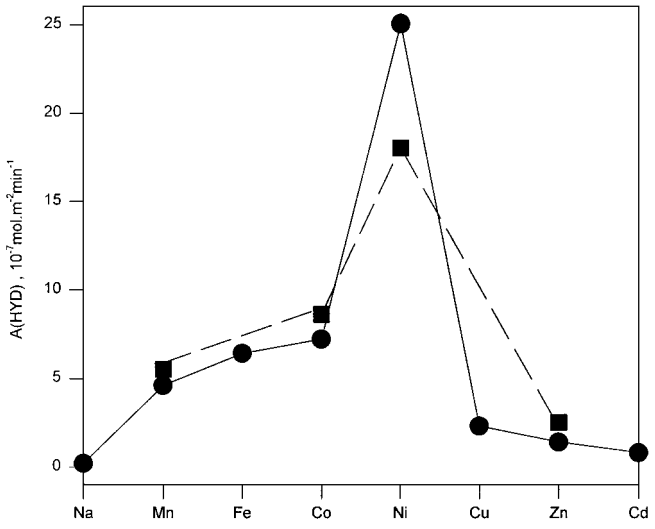

FIG. 5. Catalytic activity of the MCr_2S_4 solids at 573 K in the reaction of HYD of tetralin (circles, oxide derived samples; squares, pyridinium complexes derived catalysts).

on the enhanced hydrogenating activity of the chromium-based sulfide catalysts (20).

Mixed sulfides obtained from the pyridinium complexes showed slightly different specific activity than those obtained from the mixed oxide precursors. Small differences in chemical composition, the impurity levels, and the crystalline planes exposed can explain such variations. However, the sequence of catalytic activity remained the same whatever the preparation method. Therefore, the curves obtained are related to the intimate properties of chemical compounds rather than to some particular features of the preparation techniques.

Temperature Programmed Reduction (TPR)

Although the exact structure of the active centers of mixed sulfide catalysts is still unclear, it seems well established that coordinately unsaturated centers are necessary for catalytic activity. Such centers can be obtained by a reductive elimination of sulfur from the sulfide surface (21, 22). TPR allows us to compare the amounts of sulfur removed from the catalysts in the wide range of reduction temperatures. Therefore, TPR results give an idea of the amount of coordinatively unsaturated centers produced in the catalysts by reduction.

Here, we studied the reducibility of the MCr_2S_4 sulfides in order to compare it with the above-observed trends in catalytic activity. Whatever the solid studied, reduction was never complete at 1073 K; the chromium remained in the sulfide form, mostly as Cr_3S_4. The second metal in some cases was completely (Fe, Co, Ni) or partially (Cu) reduced and in other cases remained nonreduced (Na, Zn) (Table 3). Phase composition of the samples after TPR at 1073 K revealed strong differences in their reducibility. However, the

TABLE 3

Phase Composition of the Mixed Sulfide Samples after Reduction at 1073 K in Hydrogen and the Amounts of Sulfur (μmol · m^{-2}) Removed at 573 K ($\Delta \cdot 573$)

Initial compound	Phases XRD after reduction at 1073 K	($\Delta \cdot 573$)
$NaCrS_2$	$NaCrS_{2-x}$	2.7
$MnCr_2S_4$	MnS, Cr_3S_4	10.2
$FeCr_2S_4$	Fe, Cr_3S_4	4.4
$CoCr_2S_4$	Co, Cr_3S_4	31.4
$NiCr_2S_4$	Ni, Cr_3S_4	53.5
$CuCr_2S_4$	$CuCrS_2$, Cr_3S_4, Cu	2.8
$ZnCr_2S_4$	$ZnCr_2S_4$, ZnS, Cr_3S_4	2.5

reducibility at such a high temperature is not relevant to the catalytic properties measured at 573 K. For the sulfide reducibility to be related to the catalytic properties, it should be measured in the same temperature range. The amount of sulfur removed at 573 K (Fig. 5) varied strongly from sample to sample and was in a good correlation (except Fe sample) with the HYD/HDS activity.

Although a clear correlation between the activity and the reducibility of MCr_2S_4 systems was observed, other parameters could influence the catalytic properties of mixed sulfides. For this reason surface characterizations of the solids have been performed.

XPS Study

The first problem regarded an eventual surface segregation in the MCr_2S_4 sulfides. When different transition metals are present in a mixed compound, strong differences between surface and volume composition become possible. Surface segregation may greatly affect the catalytic activity. To clarify this point, MCr_2S_4 samples were studied by the XPS technique. Another goal of the XPS study was to obtain information on the electronic state of the components.

We studied the samples of six mixed sulfides, obtained after sulfidation of the oxide precursors. Binding energies and M/Cr surface atomic ratios are listed in Table 4. To our knowledge no systematic XPS studies of the thiospinels was

TABLE 4

XPS Binding Energies (eV) of the Elements in the MCr_2S_4 Compounds

Sample	Cr $2p_{3/2}$	S 2p	M $2p_{3/2}$	M/Cr, at.
$MnCr_2S_4$	575.4	161.4	641.9	0.25
$FeCr_2S_4$	576.9	162.9, 161.5	711.3	0.69
$CoCr_2S_4$	575.5	161.4	779.8	0.49
$NiCr_2S_4$	575.4	161.5	853.4	0.35
$CuCr_2S_4$	575.8	162.2	932.8	0.28
$ZnCr_2S_4$	576.1	162.9, 161.6	1022.3	0.17

done earlier, so we briefly comment on the observed BE values.

Chromium $2p_{3/2}$ binding energy lies above the value of 574.8 observed for Cr_2S_3 (23). The values of BE for Mn, Co, Ni, and Zn $2p_{3/2}$ levels corresponded fairly to those in MS sulfides (24). Iron showed a peak which also corresponds rather well to FeS (23), whereas no signal was found at 706.7 eV, that of the FeS_2 impurity (25).

Unfortunately, the binding energy of 932.8 eV obtained for Cu $2p_{3/2}$ was not helpful for conclusions about the copper oxidation state, due to too much discrepancy in the literature data on Cu sulfides. Indeed, a binding energy of 932.5 eV was reported for Cu_2S (26), but those for CuS varied from 931.9 (27) to 935.0 eV (28).

For mixed Co and Ni sulfides obtained from the pyridinium complexes at 673 K, the sulfur signals consisted of two components. Two signals with BE of ca. 162.8 and 161.5 were ascribed to, respectively, $(S_2)^{2-}$ and S^{2-} species, as reported previously (29, 30). After sulfidation at 873 K only a low-energy component remains.

From the analysis of the surface composition it can be concluded that most of the samples are slightly enriched with chromium, with the exception of the Fe sample, where a small excess of Fe was present (Table 4). The degree of enrichment somewhat varied, but the surface Cr concentration was systematically higher than its bulk value. We see that the M/Cr atomic ratio varied from 0.17 to 0.69, whereas catalytic activity in the same samples differed by more than an order of magnitude. Therefore, we suggest that catalytic activity variations are not related to surface segregation but to the differences in the chemical nature of the solids.

LEIS Study

Although the enrichment of the samples with chromium was observed by XPS, it can still not be stated which element predominates in the very topmost surface layer under the conditions of catalytic reaction since, depending on the escape depth, the XPS analysis of the surface gives information on the layer of the thickness of 2–10 nm, i.e., several atomic layers. For this reason low-energy ion scattering study was undertaken to obtain information regarding the very topmost atomic layers of our solids.

With 1 KeV $^4He^+$ incident ions, Co, Fe, and Mn signals could not be distinguished from that of Cr. We studied therefore Ni-, Zn-, and Cu- containing solids, for which the LEIS signals of transition metals are well separated.

The results of LEIS as a function of sputtering time are presented in Fig. 6 for Cu and Ni. In all cases the behavior of samples upon sputtering is similar. Although the quantitative interpretation of LEIS data is difficult, the intensity of peaks is roughly proportional to the amount of the corresponding elements. The intensities of transition metals signals in the first scan before sputtering appear to be in contradiction with the XPS data. The intensity of the chromium signal was lower than that of M(II). Then, upon stuttering, the intensity of the Cr peak rapidly increased, becoming several times higher than that of M(II), while the first atomic layer was still not destroyed (the time for

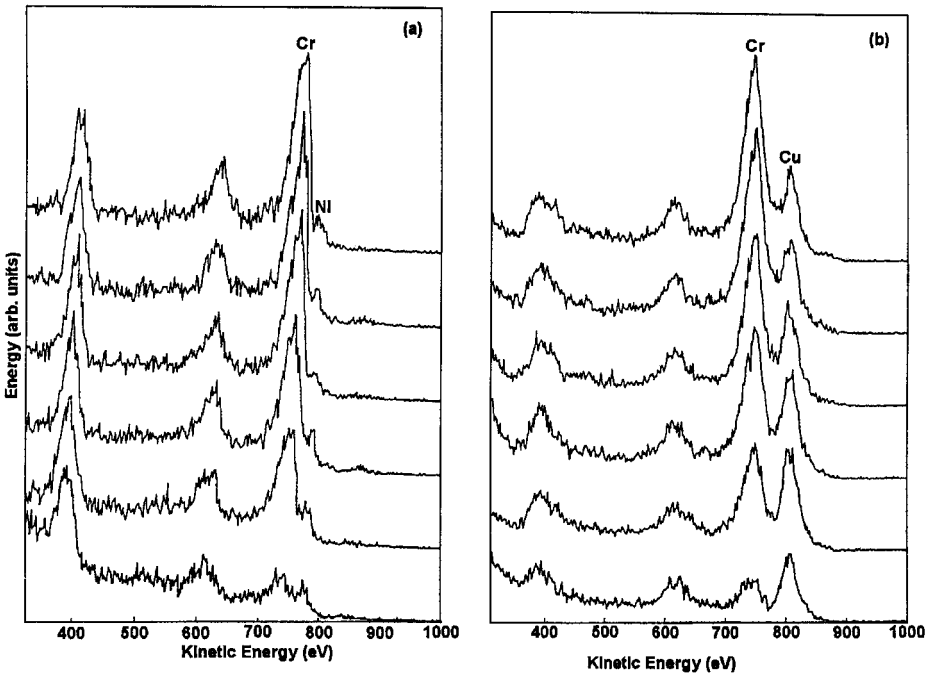

FIG. 6. LEIS profiles as a function of sputtering time of $NiCr_2S_4$ (a) and $CuCr_2S_4$ (b). The sputtering time between subsequent scans is 60 s.

monolayer removal is estimated to be ca. 600 s (31)). Therefore, being less visible at the first moment, chromium is immediately exposed upon ion bombardment, whereas the signals of M(II) ions undergo small variations vs sputtering time. The signal of sulfur is low compared to its relative amount, because of the low sensitivity of the LEIS technique to this element. The sulfur signal showed no significant evolution during sputtering. It seems that the sulfur concentration cannot be correctly studied by LEIS in our systems.

To explain the findings of both XPS and LEIS measurements, we suggest that certain low-index crystalline planes are preferentially exposed to the surface, which contains mostly Cr sites. However, in the top layer Cr atoms are efficiently screened by sulfur or some adsorbed impurity. In the spinel structure, such planes are, for example, (100) and (111) (Fig. 7). The signal of the second metal M should be due to other planes, present in lower amounts.

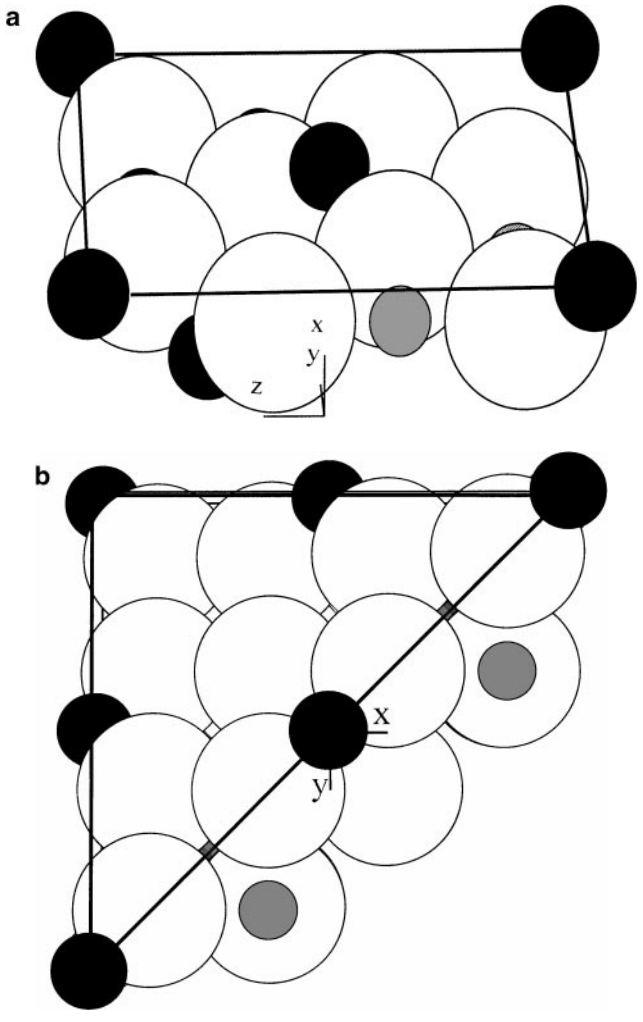

FIG. 7. Low-index planes of thiospinels (110) (a) and (111) (b). Large hollow circles, sulfur; black circles, chromium; gray circles, the second metal.

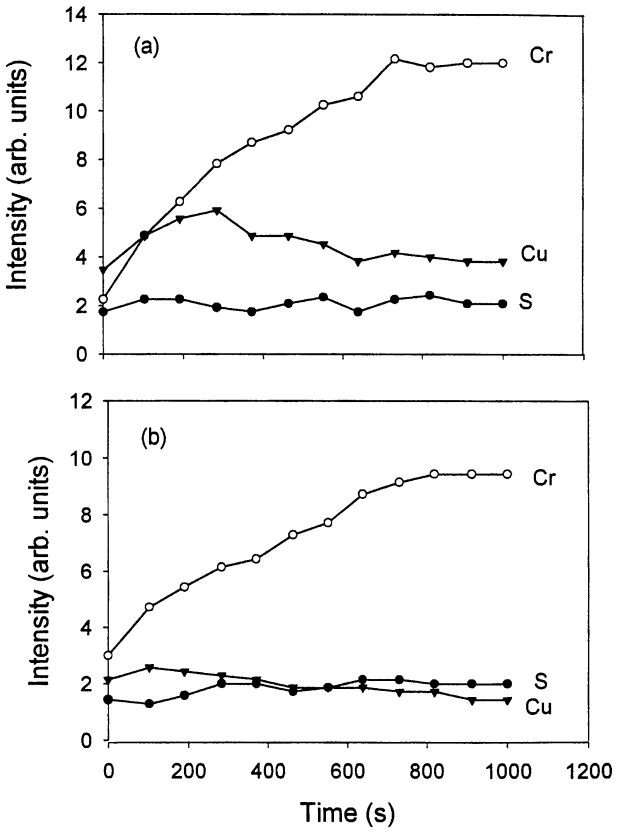

FIG. 8. Intensity of the LEIS signals vs sputtering time for the $CuCrS_2$ solid: nontreated (a) and reduced for 1 h at 573 K (b).

To clarify this question we measured the LEIS and XPS spectra of the $CuCr_2S_4$ sample after reduction in hydrogen at 573 K for 1 h. The LEIS spectrum obtained after reduction is similar to that of the nonreduced Cu sample, taken at the intermediate point of sputtering (Fig. 8). Therefore, reduction at 573 K produces the same effect in the LEIS spectra as slight sputtering. In both cases, elimination of polluting adsorbed species and the topmost layers of sulfur occurred.

From the surface chemistry of the oxide spinels, it is known that they often expose low-index crystalline planes consisting of octahedral MO_6 (32, 33). Moreover, it was proposed in these works that the absence of the occupied tetrahedral sites at the surface is a general property of spinels. Our data give additional support to this hypothesis for the case of thiospinels. It follows from our experiments that Cr is exposed to the surface upon reduction in hydrogen at 573 K. Therefore, we can suggest that coordinately unsaturated sites are located on Cr atoms.

XPS data after reduction confirm the supposition about the removal of sulfur from the chromium sites. Indeed, after reduction at 573 K, the XPS atomic ratio of Cr/Cu did not significantly change, whereas the amount of sulfur decreased from 42 to 30%. At the same time the Cr signal

undergoes a shift to lower binding energy, indicating its partial reduction from its initial value of 575.8 to 575.1 eV, clearly indicating the reduction of chromium. By contrast, the Cu XPS signal after reduction remains at the same position as in the initial specimen.

Extended Hückel Calculations

It follows from our data that the catalytic activity of the MCr_2S_4 systems is directly related to the reducibility of their surface. Depending on the nature of the second metal *M*, the strength of sulfur bonding may change, leading to variations in reducibility. To illustrate the influence of the second metal on sulfur bonding, we carried out extended Hückel calculations of the electronic structure of the mixed sulfides MCr_2S_4.

The extended Hückel method does not take into account spin polarization effects, which in the MCr_2S_4 solids should be considerable. However, in the series of similar compounds the method gives an idea of the bands filling and bonding energy changes. Moreover, the physical properties of thiospinels have been extensively studied so that the results of EH calculations might be compared with the literature data of density functional calculations.

In this work, we calculated the density of states distributions of different mixed sulfides as well as the projections of sulfur and transition metal levels, and the crystal orbital overlap population between sulfur and both metals.

The band structure of the MCr_2S_4 compounds contains filled S 3p levels, empty *M* 4p, and partially filled *M* 3d bands as schemed in Fig. 9. Since in the oxide chromite spinels (34) ground ^4F term of the Cr(III)d^3 ion has much lower energy than the P term, we believe that in thiospinels, where the crystal field is weaker, mixing with those states can be neglected. The energy of the second metal d bands relative to the chromium 3d levels changes as a function of the position in the periodic table. Electric conductivity and magnetic properties of thiospinels are determined by the energy of the second metal bands and their interaction with the Cr(III) 3d states. Thus, $FeCr_2S_4$ is a ferrimagnetic semiconductor (34); $CuCr_2S_4$ is a ferromagnetic metallic conductor (35) and $CdCr_2S_4$ is a ferromagnetic *n*-type semiconductor (36).

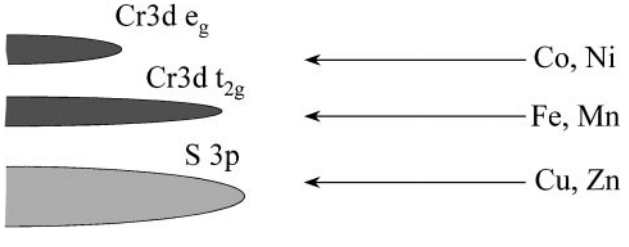

FIG. 9. Schematic energy diagram showing the relative band positions in the MCr_2S_4 compounds.

TABLE 5

EH Electronic Stabilization Energy (kcal/mol) and Metal–Sulfur Bond Lengths in the MCr_2S_4 Compounds

M	ΔE stab	d(*M*–S), Å	d(Cr–S), Å
2Na	−558	2.798	2.454
Mn	−485	2.241	2.497
Fe	−451	2.209	2.461
Co	−449	2.191	2.448
Ni	−431	2.388	2.424
Cu	−481	2.170	2.418
Zn	−489	2.211	2.463

The electronic stabilization energies obtained from the EH calculations are listed in Table 5. As expected, a pronounced minimum of the cohesion energy is obtained for Co and Ni compounds. There is no clear correlation between the sulfur binding energy and the bond lengths. It seems that a rather inverse correlation exists, i.e., long ionic bonds are stronger than short (covalent) ones. However, this correlation is also incomplete, since the Cu compound having the shortest bonds does not exhibit the lowest stabilization energy.

Below we give a brief summary of the analysis of DOS and COOP curves obtained from the EH calculations.

In the $NaCrS_2$ compound, the presence of the alkali metal leads obviously to the increase in the compound ionicity with the lowering of the S 3p states energy and increase of the total electronic stabilization energy.

For the transition metal sulfides MCr_2S_4, when *M* goes from the left to the right of the first row of the periodic table, the electronic effects observed result from the competition of two opposite trends—filling of the 3d band of *M* increasing the energy of 3d electrons and the increase of the *M* atomic number, shifting the 3d band down.

For the chromium neighbors in the periodic table, Mn and Fe, the d levels of the second metal are close to those of Cr and the effect is not clear, at least in the frames of the EH method.

Then, passing to Co, the band filling begins to predominate over the band shifting down, and the HOMO states of the mixed sulfide $CoCr_2S_4$ are probably those of Co 3d. At the same time the S–Cr and S–Co antibonding orbitals become populated due to the increased d electrons count. The same situation was observed for Ni, the effect being the decrease of sulfur binding energy. In the case of Cu, the d band, although filled, is already placed too low, and Cu introduction into the mixed sulfide results in increased sulfur bonding. Indeed, $CuCr_2S_4$ was considerably less reducible than the Co and Ni compounds.

Being at best approximate, the results of the EH calculations are, however, in surprisingly good agreement with our experimental observations and give a clear qualitative insight of the electronic effects in these systems.

Unfortunately, V and Ti have no stable *M*(II) compounds to complete the series.

Several works have been done on the calculations of electronic properties of sulfides in order to explain the trends of their catalytic activity. Harris and Chianelli compared the catalytic properties of binary sulfides of numerous transition metals and analyzed the results of *ab initio* calculation of the electronic structure of octahedral MS_6 clusters. They concluded that for a sulfide to be an active hydrotreating catalyst, its HOMO should have t_{2g} character (37). Recently Raybaud *et al.* (38) made an extensive *ab initio* calculation of the electronic structure of binary sulfides. They concluded that the energy of the metal–sulfur bond is of primary importance for the HDS catalytic activity. The density functional calculations of the electronic structure of MoS_2 and Co–Mo–S catalysts led the authors (39) to the conclusion about the key role of sulfur bonding strength. The promoting effect of Co was explained by lowering the S binding energy, thereby increasing the number of the active sites.

Here we deal with another example of mixed sulfide catalysts where the effect of promotion (if Cr stays for the "main element" and *M* for the "promoter") could be coherently explained by variations of the sulfur binding strength.

CONCLUSION

In this work we studied mixed sulfide MCr_2S_4 catalysts in HDS and HYD model reactions. These solids showed enhanced hydrogenating properties, the specific activities being sometimes comparable to that of dispersed Mo sulfide. By contrast to the industrial sulfide catalysts, which are difficult to characterize, MCr_2S_4 mixed sulfide dispersions have well-defined surface and bulk properties. Trends in catalytic activity could be easily explained from the comparison with TPR and surface characterization data. The idea of dynamically created active centers seems to get additional support in this work. Although different elementary steps of HYD and HDS catalytic reactions were not at all considered here, sulfur lability seems to be a key parameter, determining the catalyst performance in both reactions.

REFERENCES

1. Pecoraro, T. A., and Chianelli, R. R., *J. Catal.* **67**, 430 (1981).
2. Eijsbouts, S., Sudhakar, C., de Beer, V. H. J., and Prins, R., *J. Catal.* **127**, 605 (1991).
3. Eijsbouts, S., de Beer, V. H. J., and Prins, R., *J. Catal.* **127**, 619 (1991).
4. Ledoux, M. J., Michaux, O., and Agostini, G., *J. Catal.* **102**, 275 (1986).
5. Lacroix, M., Boutarfa, N., Guillard, C., Vrinat, M., and Breysse, M., *J. Catal.* **120**, 473 (1989).
6. Brostigen, G., and Kjekshus, K., *Acta Chem. Scand.* **23**, 2186 (1969).
7. Aminoff, G., *Zeit. Crystallogr.* **58**, 203 (1923).
8. Bacon, G. E., *Zeit. Crystallogr.* **82**, 325 (1932).
9. Brongersma, H. H., and Van Leerdam, G. C., "Fundamental Aspects of Heterogeneous Catalysis Studied by Particle Beams," p. 283. Plenum Press, New York, 1991.
10. Delichère, P., Béré, K. E., and Abon, M., *Appl. Catal. A Gen.* **172**, 295 (1998).
11. Brandle, M., Rytz, R., and Calzaferri, G., "BICON–CEDiT Extended Hückel Band Structure and Crystal Electronic Dipole Induced Transitions Calculations." Bern, 1997. Available at the site.
12. Summerville, R. H., and Hoffmann, R., *J. Am. Chem. Soc.* **98**, 7240 (1976).
13. Calzaferri, G., and Felix, F., *Helv. Chim. Acta* **60**, 730 (1977).
14. Hay, P. J., Thibeault, J. C., and Hoffmann, R., *J. Am. Chem. Soc.* **97**, 4884 (1975).
15. Lauher, J. W., Elian, M., Summerville, R. H., and Hoffmann, R., *J. Am. Chem. Soc.* **98**, 3219 (1976).
16. Viste, A., Hotokka, M., Laaksonen, L., and Pyykko, P., *Chem. Phys.* **72**, 225 (1982).
17. Kanatzidis, M. G., and Sutorik, A. C., "Progress in Inorganic Chemistry, Vol. 43" (K. D. Karlin, Ed.), p. 151. Wiley, New York, 1995.
18. Ruedorf, W., and Stegemann, K., *Zeit. Anorg. Allg. Chem.* **251**, 376 (1943).
19. Andron, B., and Bertaud, J., *J. Phys.* **27**, 619 (1966).
20. Thiollier, A., Afanasiev, P., Cattenot, M., and Vrinat, M., *Catal. Lett.* **55**(1), 39 (1998).
21. Lacroix, M., Jobic, H., Dumonteil, C., Afanasiev, P., Breysse, M., and Kasztelan, S., "Proceedings, 11th International Congress on Catalysis, Baltimore, 1996" (J. W. Hightower, W. N. Delgass, E. Iglesia, and A. T. Bell, Eds.), Elsevier, Amsterdam, 1996.
22. Lacroix, M., Mirodatos, C., Breysse, M., Decamp, T., and Yuan, S., "Proceedings, 10th International Congress on Catalysis, Budapest, 1992" (L. Guczi, F. Solymosi, and P. Tenenyi, Eds.). AkadémiaiKiadó, Budapest, 1993.
23. Carver, J. C., Schweitzer, G. K., and Carlson, T. A., *J. Chem. Phys.* **57**, 973 (1972).
24. Moulder, J. F., Stickle, W. F., Sobol, P. E., and Bomben, K. D., "Handbook of X-Ray Photoelectron Spectroscopy" (J. Chastain, Ed.), Perkin–Elmer, Corporation, 1992.
25. Binder, H. Z., *Naturforsch. B* **28**, 256 (1973).
26. Wagner, C. D., *Discuss. Faraday Soc.* **60**, 291 (1975).
27. Bhide, V. G., Salkalachen, S., Rastogi, A. C., Rao, C. N. R., and Hegde, M. S., *J. Phys. D* **14**, 1647 (1981).
28. Nefedov, V. I., Salyn, Y. V., Solozhenkin, P. M., and Pulatov, G. Y., *Surf. Interface Anal.* **2**, 171 (1980).
29. Vrinat, M., Guillard, C., Lacroix, M., Breysse, M., Kurdi, M., and Danot, M., *Bull. Soc. Chim. Belg.* **96**(11/12), 1017 (1987).
30. De Los Reyes, J. A., Vrinat, M., Geantet, C., Breysse, M., and Grimblot, J., *J. Catal.* **142**, 455 (1993).
31. Bertolini, J. C., Delichere, P., and Hermann, P., *Surf. Interface Anal.* **24**, 34 (1996).
32. Jacobs, J. P., Maltha, A., Reitjes, J. G. H., Drimal, J., Ponec, V., and Brongersma, H. H., *J. Catal.* **147**, 294 (1994).
33. Davies, M. J., Parker, S. C., and Watson, G. W., *J. Mater. Chem.* **4**(6), 813 (1994).
34. Freyia Fava, F., Baraille, I., Lichanot, A., Larrieu, C., and Dovesi, R., *J. Phys. Condens. Matter* **9**, 10715 (1997).
35. Ramirez, A. P., Cava, R. J., and Krajewski, J., *Nature* **386**, 156 (1997).
36. Pouget, S., and Alba, M., *J. Phys. Condens. Matter* **7**, 4739 (1995).
37. Harris, S., and Chianelli, R. R., *J. Catal.* **86**, 400 (1984).
38. Raybaud, P., Kresse, G., Hafner, J., and Toulhoat, H., *J. Phys. Condens. Matter* **9**, 11085 (1997).
39. Byskov, L. S., Hammer, B., Norskov, J., Clausen, B. S., and Topsøe, H., *Catal. Lett.* **47**, 177 (1997).